Roles of individual domains in the function of DHX29, an essential factor required for translation of structured mammalian mRNAs

Vidya Dhote, Trevor R. Sweeney, Natalia Kim, Christopher U. T. Hellen, and Tatyana V. Pestova[1]

Department of Cell Biology, State University of New York Downstate Medical Center, Brooklyn, NY 11203

Edited by Jennifer A. Doudna, University of California, Berkeley, CA, and approved September 18, 2012 (received for review May 11, 2012)

On most eukaryotic mRNAs, initiation codon selection involves base-by-base inspection of 5′ UTRs by scanning ribosomal complexes. Although the eukaryotic initiation factors 4A/4B/4G can mediate scanning through medium-stability hairpins, scanning through more stable structures additionally requires DHX29, a member of the superfamily 2 DEAH/RNA helicase A (RHA) helicase family that binds to 40S subunits and possesses 40S-stimulated nucleoside triphosphatase (NTPase) activity. Here, sequence alignment and structural modeling indicated that DHX29 comprises a unique 534-aa–long N-terminal region (NTR), central catalytic RecA1/RecA2 domains containing a large insert in the RecA2 domain, and the C-terminal part, which includes winged-helix, ratchet, and oligonucleotide/oligosaccharide-binding (OB) domains that are characteristic of DEAH/RHA helicases. Functional characterization revealed that specific ribosomal targeting is required for DHX29's activity in initiation and is determined by elements that map to the NTR and to the N-terminal half of the winged-helix domain. The ribosome-binding determinant located in the NTR was identified as a putative double-stranded RNA-binding domain. Mutational analyses of RecA1/RecA2 domains confirmed the essential role of NTP hydrolysis for DHX29's function in initiation and validated the significance of a β-hairpin protruding from RecA2. The large RecA2 insert played an autoinhibitory role in suppressing DHX29's intrinsic NTPase activity but was not essential for its 40S-stimulated NTPase activity and function in initiation. Deletion of the OB domain also increased DHX29's basal NTPase activity, but more importantly, abrogated the responsiveness of the NTPase activity to stimulation, which abolished DHX29's function in initiation. This finding suggests that the OB domain, which is specific for DEAH/RHA helicases, plays an important role in their NTPase cycle.

DEAH/RHA family | translation initiation

Translation initiation on the majority of eukaryotic mRNAs occurs by the scanning mechanism (1). First, 43S preinitiation complexes comprising 40S subunits, Met-tRNA$_i^{Met}$/eIF2/GTP, and eukaryotic initiation factors (eIFs) 3, 1, and 1A attach to the cap-proximal region of mRNA in a process that is mediated by eIF4A, eIF4B, and eIF4F. eIF4F consists of three subunits: eIF4E (a cap-binding protein), eIF4A (a DEAD-box RNA helicase), and eIF4G (a scaffold for eIF4E and eIF4A, which also binds to eIF3). eIFs 4A/4B/4G cooperatively unwind the cap-proximal region of mRNA allowing attachment of 43S complexes. After attachment, 43S complexes scan to the initiation codon where they form 48S initiation complexes with established codon–anticodon base-pairing. In addition to promoting attachment, eIFs 4A/4B/4G assist 43S complexes during scanning. Although eIFs 4A/4B/4G can mediate scanning through stems of medium stability, scanning through more stable secondary structures additionally requires the DExH-box protein DHX29 (2). DHX29 is also essential for initiation on several viral mRNAs (3, 4). Consistent with its important role in initiation, silencing of DHX29 inhibits general translation, resulting in polysome disassembly and accumulation of mRNA-free 80S ribosomes, and impedes cancer cell growth (5).

Interestingly, in the absence of DHX29, intact stems are not prevented from entering the mRNA-binding channel of scanning 43S complexes. However, they cannot be threaded through its exit portion, resulting in incorrect positioning of mRNA upstream of the P site, which renders 48S complexes formed on AUGs downstream of intact stems susceptible to dissociation by eIF1 (6). On the other hand, in 48S complexes formed on AUGs immediately preceding intact stable stems, the stem and an adjacent mRNA region between the stem and the AUG are accommodated in the A site, and such complexes are dissociated by DHX29 (6). DHX29 also suppresses formation of aberrant 48S complexes characterized by the +8–9–nt toe-prints, in which the mRNA is not accommodated along the entire entry portion of the mRNA-binding channel (2). Importantly, DHX29 not only dissociates 48S complexes in which mRNA is not properly accommodated downstream of the P-site but also promotes unwinding of stems at the mRNA entrance, ensuring that mRNA is subjected to linear inspection during scanning (6).

DHX29 binds to 40S subunits near the mRNA entrance, likely contacting helix 16 of 18S rRNA, and has a nucleoside triphosphatase (NTPase) activity that is strongly stimulated by 40S subunits (2). Although the ribosomal position of DHX29 would allow it to unwind mRNA directly before it enters the mRNA-binding cleft, DHX29 is not a processive helicase, and its NTPase activity is stimulated more strongly by 43S complexes than by RNA (2). These properties of DHX29, together with its ability to dissociate aberrant 48S complexes with mRNA incorrectly positioned in the entry portion of the mRNA-binding channel, suggest that it likely acts by remodeling ribosomal complexes. Cycling between NTP- and NDP-bound states, DHX29 might induce opening and closing of the mRNA entry channel, which could indirectly help 43S complexes to unwind entering stems. However, the possibility that association with 43S complexes might enhance DHX29's helicase activity cannot strictly be excluded; in that case it also may participate in direct unwinding. Interestingly, DHX29 stimulates 48S complex formation most strongly when it is present in substoichiometric amounts relative to 43S complexes and can participate in multiple rounds of 48S complex formation (2). However, the stage at which DHX29 dissociates from ribosomal complexes is not known.

DHX29 belongs to the RNA helicase A (RHA) subfamily of superfamily 2 (SF2) DEAH/RHA RNA helicases. Other mammalian DEAH helicases include DHX16, DHX38, DHX8, DHX15 (in yeast, Prp2p, Prp16p, Prp22p, and Prp43p, respectively) and DHX35. The RHA-like group comprises RHA (also called "DHX9"), DHX30, DHX36, and DHX57 (http://www.rnahelicase.org). Like other SF2 (as well as SF1) helicases, DEAH/RHA helicases possess a catalytic core comprising tandem RecA-like domains, containing characteristic motifs (I–VI) that are involved

Author contributions: V.D., T.R.S., C.U.T.H., and T.V.P. designed research; V.D., T.R.S., and N.K. performed research; V.D., T.R.S., C.U.T.H., and T.V.P. analyzed data; and C.U.T.H. and T.V.P. wrote the paper.

The authors declare no conflict of interest.

This article is a PNAS Direct Submission.

[1]To whom correspondence should be addressed. E-mail: tatyana.pestova@downstate.edu.

See Author Summary on page 18641 (volume 109, number 46).

This article contains supporting information online at www.pnas.org/lookup/suppl/doi:10.1073/pnas.1208014109/-/DCSupplemental.

in ATP-binding/hydrolysis, RNA-binding, and coupling of ATP hydrolysis with nucleic acid unwinding. A unique feature of the DEAH/RHA family is the presence of a conserved C-terminal region following the helicase core. The structure of ADP-bound Prp43p, which is involved in ribosome biogenesis and mRNA splicing, identified three distinct domains in this region: a winged-helix (WH) domain that interacts closely with the RecA1 domain, a ratchet domain (a seven-helix bundle that binds across both RecA domains), and a β-barrel oligonucleotide/oligosaccharide-binding (OB) domain that is connected to the ratchet domain by an α-helix (7, 8). The WH and ratchet domains of Prp43p are homologous to the corresponding domains in the archaeal Ski2-like DNA helicase Hel308, which is involved in DNA repair (9), whereas the C-terminal OB domain is specific for the DEAH/RHA family. Additionally, unlike DEAD-box helicases but like Hel308, Prp43p has a prominent antiparallel β-hairpin protruding from its RecA2 domain between motifs V and VI. The structural homology between Hel308 and Prp43p led to the proposal that Prp43p (and by analogy all DEAH/RHA RNA helicases) also may function by a mechanism of processive translocation suggested for Hel308 (9), in which the β-hairpin acts as a wedge for separating the strands of a duplex nucleic acid, and the long ratchet helix of the ratchet domain interacts with the bases of the unwound single strand and facilitates its translocation through the nucleic acid-binding cavity.

To investigate the mechanism of DHX29's action, we generated a DHX29 model, using the crystal structure of Prp43p, and determined the role of individual domains of DHX29 in ribosomal binding, NTP hydrolysis, and 48S complex formation on structured mRNAs.

Results

Structural Modeling of DHX29. Although the N-terminal region (NTR; amino acids 1–534) of DHX29 showed no homology to any particular class of proteins, BLAST searches and sequence alignment (Fig. 1*A*) revealed that the C-terminal two thirds (amino acids 535–1369) are strongly homologous to the RecA, WH, ratchet, and OB domains of Prp43p and RHA. These regions of DHX29 and Prp43p share 30.5% sequence identity and 22% conservative substitutions, and if the predicted insert 1 in DHX29 is excluded, these values increase to 36% and ~26%, respectively. The Prp43p crystal structure (Fig. 1*B*) (7, 8) therefore could be used as a template to generate a DHX29 model. In support of this strategy, comparison of the RecA1 domains of Prp43p [Protein Data Bank (PDB) ID: 3KX2] (7) and RHA (PDB ID: 3LLM) (10), which share 39% sequence identity and 25% conservative substitutions, showed that their structures are highly conserved (*SI Appendix*, Fig. S1). Similarly, the WH, ratchet and OB domains of Prp22p (PDB ID: 3I4U) and Prp43p (PDB ID: 3KX2), which share 70% sequence similarity, adopt very similar folds (*SI Appendix*, Fig. S1).

To generate a DHX29 model, residues 541–1369 of DHX29 were submitted to the SwissModel server, using Prp43p's structure as a template. The resulting model includes residues 551–1302 of DHX29 (Fig. 1*C*) and features RecA1 (amino acids 551–757) and RecA2 (amino acids 758–1007) domains, which share 70% and 73% sequence similarity with the equivalent domains in Prp43p if the predicted insert 1 in DHX29 (amino acids 768–843) is excluded, as well as WH (amino acids 1008–1077), ratchet (amino acids 1078–1193) and OB (amino acids 1228–1289) domains, with residues 1167–1190 forming the ratchet helix. Like Prp43p, DHX29 has a prominent antiparallel β-hairpin protruding from between motifs V and VI of the RecA2 domain. DHX29-specific inserts (Fig. 1*A*) occur in loops connecting conserved secondary structure elements (dotted lines in Fig. 1*C*).

The region C-terminal to the OB domain in DHX29 is substantially longer than in Prp43p (Fig. 1*A*) and is more similar to the equivalent region in RHA-like helicases than to the region in Prp43p (*SI Appendix*, Fig. S2). Moreover, unlike Prp43p but like other RHA-like helicases, DHX29 also contains a large insert between the β1 strand and α1 helix of the RecA2 domain (Fig. 1*A* and *SI Appendix*, Fig. S3). The potential structure of these regions of DHX29 is discussed below.

Roles of DHX29's NTR, Central RecA Domains, and C-Terminal Region in Ribosomal Binding, NTP Hydrolysis, and 48S Complex Formation. To determine the contributions of the DHX29-specific NTR (amino acids 1–534), the central RecA domains (amino acids 535–1007), and the C-terminal region (amino acids 1008–1369) to specific activities of DHX29, N- and C-terminally truncated DHX29 mutants (Fig. 2*A*) were expressed and purified from *Escherichia coli*. To assay ribosomal binding, the mutants were incubated with 40S subunits, Met-tRNA$_i^{Met}$, and eIFs 2/3/1/1A, and reaction mixtures then were subjected to sucrose density gradient (SDG) centrifugation. The presence of DHX29 in SDG fractions corresponding to 43S complexes was analyzed by SYPRO staining or by Western blotting if DHX29 fragments comigrated with eIFs or ribosomal proteins. The NTR and the C-terminal region, but not the central RecA domains, associated with 43S complexes (Fig. 2*B*, first two panels on the left). C-terminal extension of the RecA domains by 32 residues yielded a polypeptide (amino acids 535–1039) that was able to bind to 43S complexes, whereas N-terminal truncation of the C-terminal region by 34 residues (amino acids 1042–1369) abrogated its ability to do so (Fig. 2*B*, second panel from the left). Thus, at least two sites in DHX29 are involved in ribosomal binding: one in the NTR, and one in the N-terminal portion of the WH domain (amino acids 1008–1039). Consistently, mutants comprising either the NTR and RecA domains or the RecA domains and the C-terminal region (amino acids 1–1039 and 535–1369, respectively) also associated with 43S complexes (Fig. 2*B*, two panels on the right).

The NTPase activity of DHX29 mutants was assayed in the presence of 40S subunits or of a U_{70} oligoribonucleotide (Fig. 2*C*). Consistent with the previous report that the NTPase activity of DHX29 is stimulated more strongly by ribosomal complexes than by single-stranded RNA (ssRNA) (2), the NTPase activity of full-length DHX29 was stimulated strongly by 40S subunits and slightly less so by U_{70} (*SI Appendix*, Fig. S4). DHX29 fragments comprising the NTR and RecA domains or RecA domains alone lacked NTPase activity (Fig. 2*C*, *Top* and *Middle*), indicating that the C-terminal region is essential for it. In contrast, deletion of the NTR reduced but did not abrogate DHX29's NTPase activity (Fig. 2*C*, *Bottom*). Interestingly, the NTPase activity of this mutant was lower than that of the full-length protein, not only in the presence of 40S subunits but also in the presence of U_{70}, suggesting that the NTR is not only required for specific binding of DHX29 to 40S subunits but also generally affects its NTPase activity. We note that the NTPase activity of the N-terminally truncated DHX29 was assayed using CTP because the protein preparation contained contaminants that elevated the background level of ATP hydrolysis.

The activity of DHX29 mutants in 48S complex formation was analyzed in an in vitro reconstituted translation system using a model (AUG at −6)-Stem mRNA comprising a GUS reporter and a 5′ UTR containing a stable stem and three AUG codons: the first at position −6 relative to the stem, the second in the loop of the stem, and the third 21 nt downstream of the stem (Fig. 2*D*) (6). In the absence of DHX29, 48S complexes form on AUG triplets immediately preceding stable stems without their unwinding; in that case intact stems are accommodated in the ribosomal A-site, and as a result such complexes are characterized by aberrant toe-prints +11–12 nt downstream of the stem (6). DHX29 promotes unwinding of stems, which results in assembly of 48S complexes with canonical toe-prints +15–17 nt downstream of the AUG triplet (6). Consistently, without DHX29, 48S complexes that formed on the AUG preceding the stem yielded toe-prints +11–12 nt downstream of the stem (Fig. 2*E*, lane 2), whereas 48S complexes formed on this AUG in the presence of full-length DHX29 yielded canonical +16–17–nt toe-prints (Fig. 2*E*, lane 3). In the latter case, a small amount of 48S complexes also formed on the two downstream AUGs. DHX29 fragments comprising either the NTR and RecA domains or RecA domains alone were inactive in 48S complex formation, and only complexes with aberrant toe-prints formed in their presence (Fig. 2*E*, lanes 5 and 6). In contrast, DHX29 lacking the NTR retained low-level activity and promoted assembly of a small amount of 48S complexes on the AUG preceding

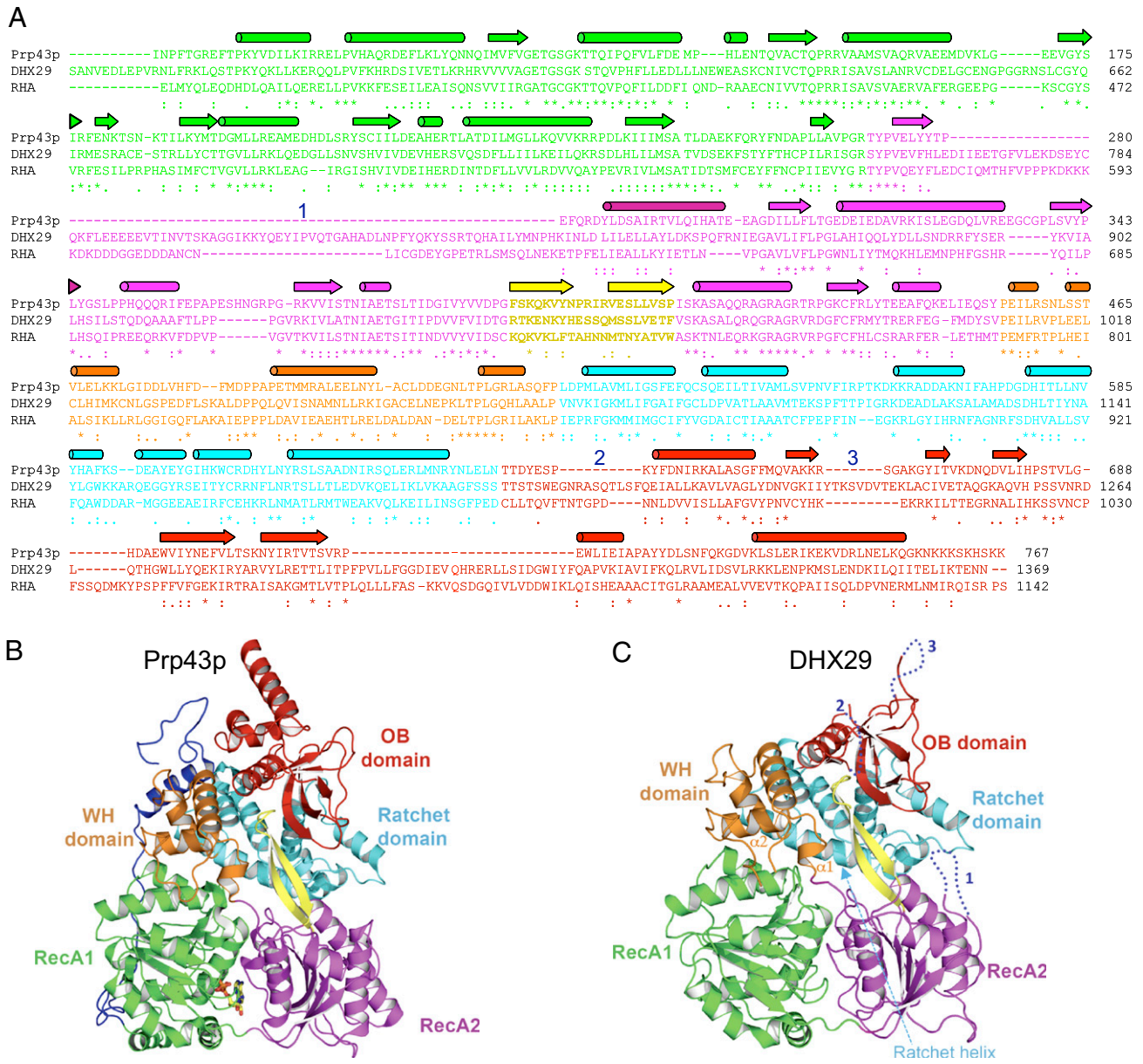

Fig. 1. Structural modeling of DHX29. (*A*) Alignment of amino acid sequences of human DHX29, *Saccharomyces cerevisiae* Prp43p, and human RHA annotated to show secondary structure elements in Prp43p (cylinders represent α-helices; arrows represent β-strands). Elements marked 1–3 are inserts present in DHX29 relative to Prp43p. (*B*) Structure of ADP-bound Prp43p in ribbon representation; ADP is shown in sticks (PDB ID: 3KX2). (*C*) Ribbon diagram of the predicted structure of DHX29 (amino acids 551–1302) generated by the SwissModel server, using the Prp43p crystal structure as a template. Corresponding domains in Prp43p (*B*) and DHX29 (*C*) are shown in the same colors as in *A*. α1 and α2 helices of the WH domain and the ratchet helix are indicated.

the stem, with canonical +16–17–nt toe-prints, and on the two downstream AUGs (Fig. 2*E*, lane 4).

In conclusion, the C-terminal region containing WH, ratchet, and OB domains is essential for DHX29's NTPase activity and for its function in 48S complex formation. Deletion of the DHX29-specific NTR, which contains determinants for ribosomal binding, does not abrogate but does very strongly impair DHX29's ability to stimulate 48S complex formation and also reduces its NTPase activity, indicating that this region is required for optimal DHX29 function.

NTR Contains a Putative dsRNA-Binding Domain That Is Required for Ribosomal Association and 48S Complex Formation. Examination of the DHX29-specific NTR for the presence of structural motifs using the PHYRE server (11) led to the identification in its C-terminal half of a dsRNA-binding domain (dsRBD) (amino acids 377–448) (Fig. 3*A*). This region is highly conserved across mammals, birds, amphibians, fish, and reptiles (*SI Appendix*, Fig. S5). The dsRBD adopts a compact αββββα fold and frequently occurs in RNA-binding proteins (e.g., ref. 12). We modeled DHX29's dsRBD (Fig. 3*B*, *Left*) on the basis of the solution structure of the related dsRBD from the mouse tRNA dihydrouridine synthase 2-like protein (PDB ID: 1WHN). In the *Drosophila* Staufen dsRBD3–RNA hairpin complex, the dsRBD's interaction with RNA is mediated by α1, β1/β2 loop 2, and β3/α2 loop 4 (Fig. 3*B*, *Right*) (13), as is typical for this domain (12).

To investigate the role of the putative dsRBD in DHX29 function, it was replaced by five alanines ($DHX29_{379–456->5Ala}$) or by a 10-aa–long linker consisting of Ala, Gly, Ser, and Thr residues ($DHX29_{379–456->10a.a.}$). In both cases, deletion of the dsRBD abrogated binding of DHX29 to 43S complexes (shown for $DHX29_{379–456->5Ala}$ in Fig. 3*C*, *Left*), indicating its essential role

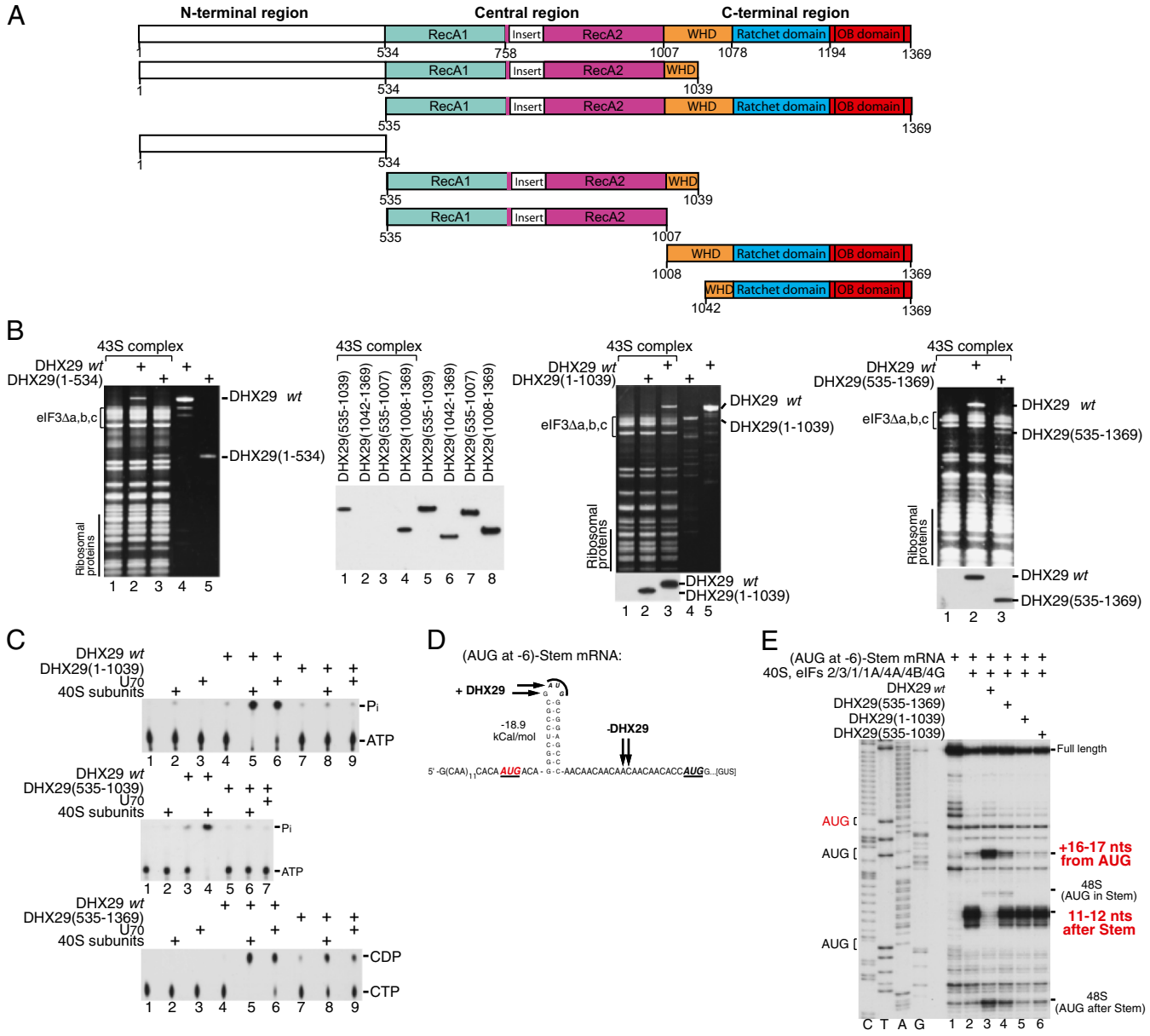

Fig. 2. The role of N-terminal, central, and C-terminal regions of DHX29 in ribosomal binding, NTP hydrolysis, and 48S complex formation. (*A*) Diagram of DHX29 deletion mutants showing domain organization (colors correspond to those used in Fig. 1). (*B*) Association of WT and mutant DHX29 with 43S complexes assembled from 40S subunits, Met-tRNA$_i^{Met}$, and eIFs 2/3/1/1A; after incubation with DHX29, ribosomal complexes were separated by SDG centrifugation, and DHX29's presence in ribosomal peak fractions was analyzed by SDS/PAGE and fluorescent SYPRO staining (left to right: first, third, and fourth panels) and/or Western blotting using DHX29 or FLAG-tag antibodies (second, third, and fourth panels). (*C*) TLC analysis of the NTPase activity of DHX29 deletion mutants in the presence of 40S subunits and U_{70} RNA. The positions of [^{32}P]-ATP, [^{32}P]-P$_i$, [^{32}P]-CTP, and [^{32}P]-CDP are shown on the right. (*D*) Sequence of the 5′ UTR of "(AUG at −6)-Stem" mRNA, containing an AUG triplet 6 nt before the stem and two other AUG triplets, in the loop of the stem and 21 nt downstream from it, respectively. Positions of toe-prints that were observed with/without DHX29 are indicated by arrows. (*E*) Toe-printing analysis of the activity of DHX29 deletion mutants in promoting 48S complex formation on (AUG at −6)-Stem mRNA. Initiation codons and the positions of full-length cDNA and of assembled ribosomal complexes are shown on the sides of each panel. Lanes C/T/A/G depict the corresponding DNA sequence.

in ribosomal association. However, the dsRBD alone did not bind stably to 43S complexes (Fig. 3*C*, *Right*), suggesting that additional elements in DHX29's NTR contribute to its stable interaction with 40S subunits. Consistent with the effect on ribosomal binding, deletion of the dsRBD led to specific loss of stimulation of DHX29's NTPase activity by 40S subunits but did not affect stimulation by U_{70} (Fig. 3*D*). Both mutants also were inactive in 48S complex formation, and in their presence only initiation complexes with aberrant toe-prints were assembled on the AUG codon preceding the stem (Fig. 3 *E* and *F*).

On the basis of structural and mutational analyses of the interaction of Staufen dsRBD3 and of PKR dsRBD1 with RNA (13, 14), we identified residues in DHX29's putative dsRBD that might be involved in interaction with 18S rRNA (Fig. 3*B*, *Left*). Four of them, K380 and F382 in helix α1 and R406 and W408 in loop 2 between β1 and β2 strands, were individually substituted by alanines, and the activity of the resulting mutants was tested in 48S complex formation. Although R406 or W408 substitutions did not affect DHX29's activity (Fig. 3*G*), replacement of K380 or F382 reduced it slightly, as was apparent by low-level assembly

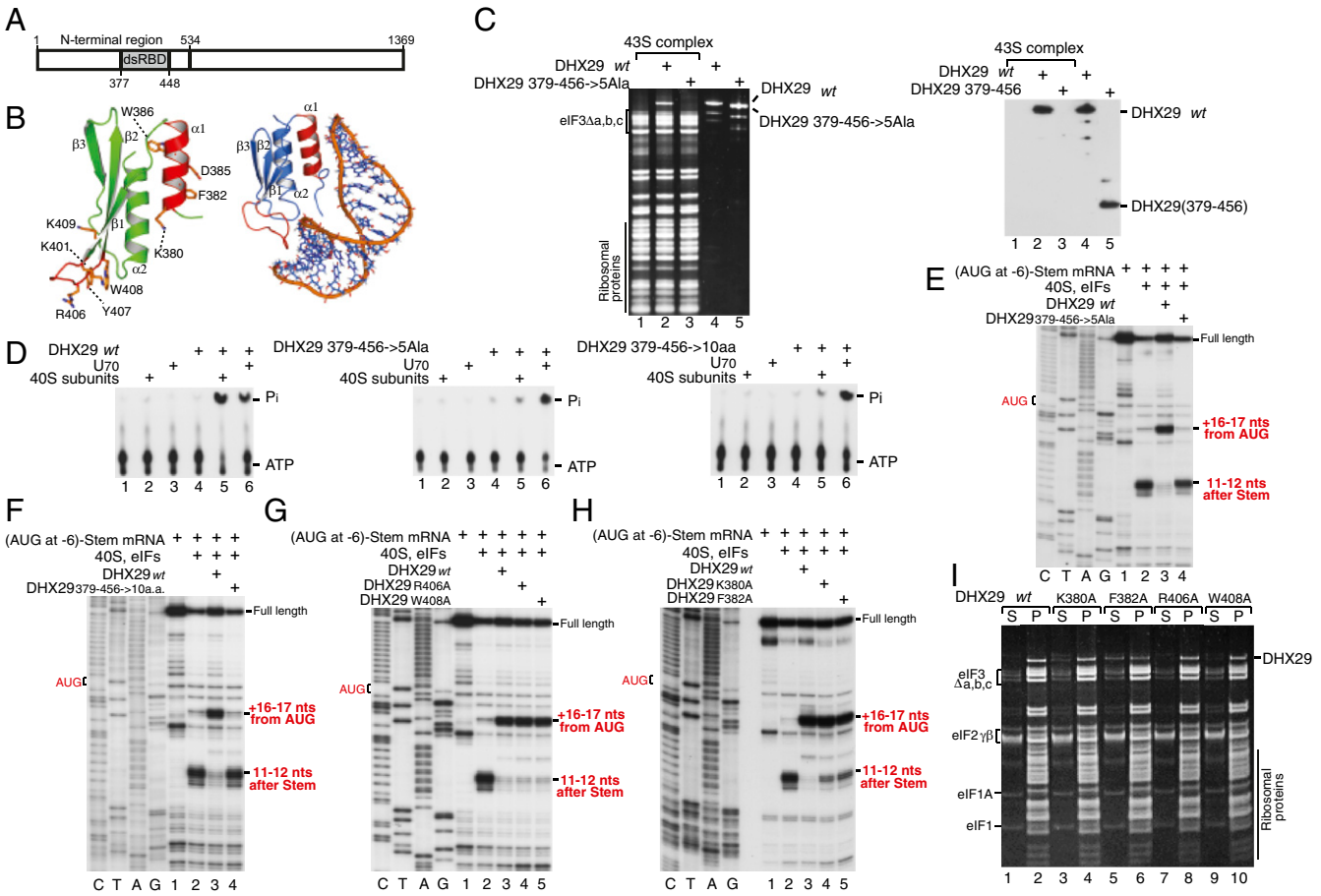

Fig. 3. A putative dsRBD in the N-terminal region is required for DHX29's association with 40S subunits and its function in 48S complex formation. (*A*) Diagram of DHX29 showing the position of the putative dsRBD. (*B*) (*Left*) Ribbon diagram of the predicted structure of DHX29's putative dsRBD (amino acids 377–448) generated using the PHYRE server, as indicated in the text. Residues potentially involved in the interaction of the dsRBD with 18S rRNA are labeled. (*Right*) The structure of *Drosophila* Staufen dsRBD3–RNA complex (PDB ID: 1EKZ). (*C*) Association of DHX29 lacking the putative dsRBD (*Left*) and of the individually expressed dsRBD (*Right*) with 43S complexes. After incubation with DHX29, ribosomal complexes were separated by SDG centrifugation, and the presence of DHX29 in ribosomal peak fractions was analyzed by SDS/PAGE and fluorescent SYPRO staining (*Left*) or Western blotting using FLAG-tag antibodies (*Right*). (*D*) TLC analysis of the NTPase activity of DHX29 dsRBD mutants in the presence of 40S subunits and U_{70} RNA. The positions of [^{32}P]-ATP and [^{32}P]-P_i are shown on the right. (*E–H*) Toe-printing analysis of the activity of DHX29 dsRBD mutants in promoting 48S complex formation on (AUG at −6)-Stem mRNA. Initiation codons and the positions of full-length cDNA and of assembled ribosomal complexes are shown on the sides of each panel. Lanes C/T/A/G depict the corresponding DNA sequence. (*I*) Association of DHX29 dsRBD mutants with 43S complexes assembled from 40S subunits and eIFs 2/3/1/1A. After incubation, reaction mixtures were centrifuged through a 10% sucrose cushion, and DHX29's presence in the supernatant and ribosomal pellet was analyzed by SYPRO staining. WT DHX29 was used as a positive control.

of 48S complexes with aberrant toe-prints (Fig. 3*H*). To assay the relative ribosomal-binding activity of these mutants, centrifugation through a 10% sucrose cushion was used. DHX29 mutants, 40S subunits, Met-tRNA$_i^{Met}$, and eIFs 2/3/1/1A were incubated at concentrations used for 48S complex formation and then were subjected to centrifugation. The presence of DHX29 in supernatant or pellet was analyzed by SYPRO staining. K380A and particularly F382A mutants (but not R406A or W408A mutants) showed reduced ribosomal binding: In contrast to the WT protein, substantial amounts of K380A and F382A mutants were present in the supernatant (Fig. 3*I*). K380 and F382 are both conserved residues (*SI Appendix*, Fig. S5). The small effect of individual substitutions in the dsRBD on DHX29's activity might be explained by the potential stabilizing influence of other elements in DHX29 on its ribosomal association.

Mutational Analysis of the RecA Domains. To confirm the requirement of NTP hydrolysis for DHX29's function, key residues within motifs I, II, III, V, and VI of the RecA domains were replaced (Fig. 4*A*). Mutations in motifs I, II, and V eliminated DHX29's NTPase activity (Fig. 4*B*) and abrogated its function in 48S complex formation (Fig. 4*F*, lanes 4–6 and 9). All mutants retained the ability to bind to 43S complexes at factor conditions used for 48S complex formation, which was assayed by centrifugation through a sucrose cushion (Fig. 4*C*). Substitution of R984 in motif VI, which is equivalent to Prp43p's R430 that forms hydrogen bonds with hydroxyl groups of the ADP's ribose moiety (8), also impaired DHX29's NTPase activity (Fig. 4*B*) and its function in 48S complex formation (Fig. 4*F*, lane 12). In contrast, the R981A substitution in the same motif showed no effect (Fig. 4*D*, lanes 7–9 and Fig. 4*F*, lane 11). Although the ability of all these mutants to hydrolyze NTP correlated with their activity in 48S complex formation, a SAT→DGD mutant in motif III, which is considered to couple NTP hydrolysis with nucleic acid unwinding (e.g., ref. 15), retained ~65% of WT NTPase activity (Fig. 4*E*) but was inactive in 48S complex formation (Fig. 4*G*). Single-substitution mutants in motif III (S734A and T736A) had no effect (Fig. 4*D*, lanes 10–15 and Fig. 4*F*, lanes 7 and 8).

In the structure of ADP-bound Prp43p, the top of the β-hairpin protruding from the RecA2 domain is inserted between the WH and OB domains, thus providing a link between the RecA domain and the C-terminal part of the protein (Fig. 1*B*) (7, 8). Y402 at the

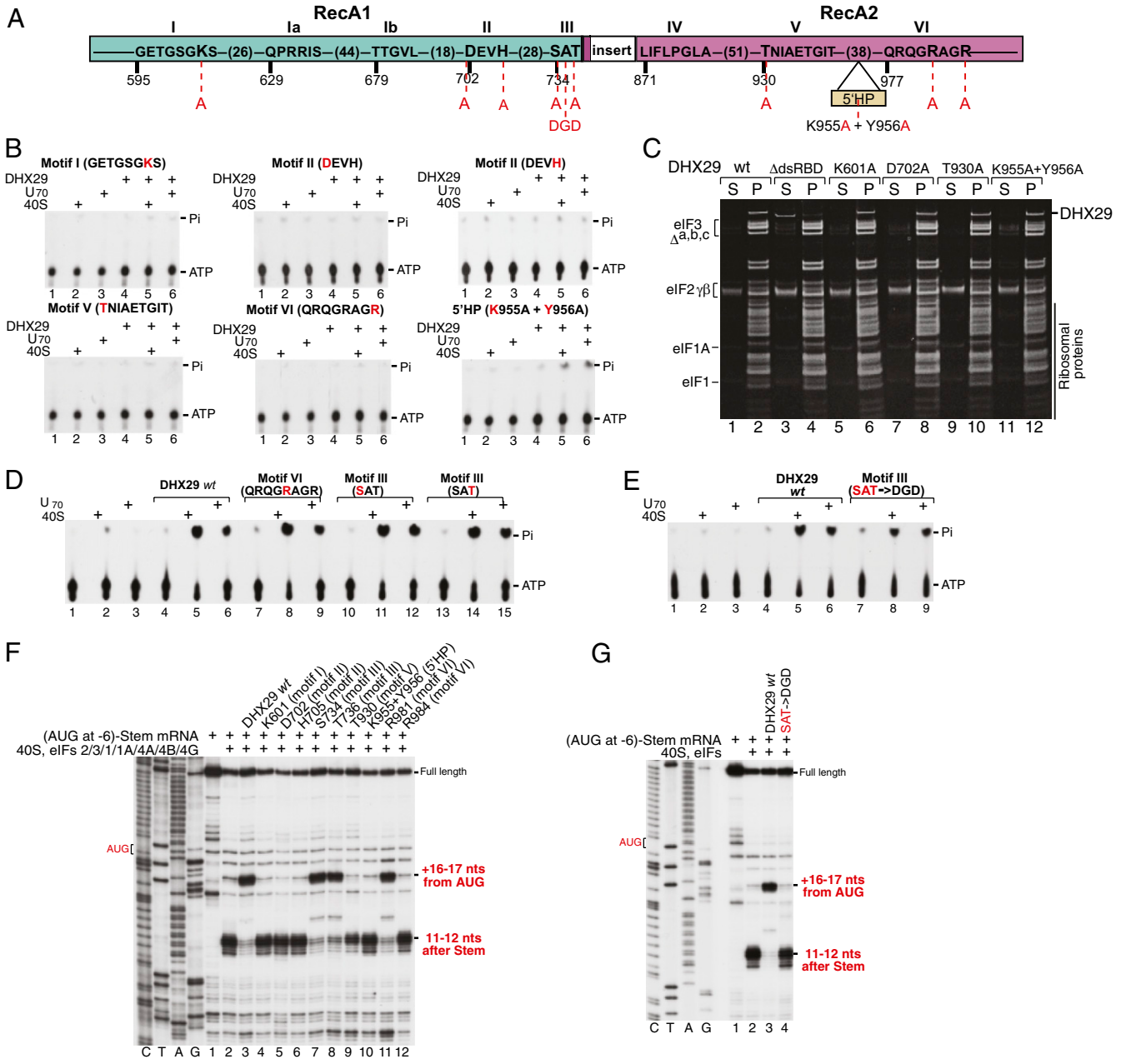

Fig. 4. Mutational analysis of the RecA domains of DHX29. (*A*) Diagram of DHX29 showing substitutions introduced into conserved motifs of the RecA domains. (*B*, *D*, and *E*) TLC analysis of the NTPase activity of DHX29 RecA mutants in the presence of 40S subunits and U_{70} RNA. The positions of [^{32}P]-ATP and [^{32}P]-P_i are shown on the right. Mutated residues are in red. (*C*) Association of DHX29 RecA mutants with 43S complexes assembled from 40S subunits and eIFs 2/3/1/1A. After incubation, reaction mixtures were centrifuged through a 10% sucrose cushion, and DHX29's presence in the supernatant and ribosomal pellet was analyzed by SYPRO staining. WT DHX29 and DHX29$_{379–456->5Ala}$ (ΔdsRBD) mutant were used as positive and negative controls, respectively. (*F* and *G*) Toe-printing analysis of the activity of DHX29 RecA mutants in promoting 48S complex formation on (AUG at –6)-Stem mRNA. Initiation codons and the positions of full-length cDNA and of assembled ribosomal complexes are shown on the sides of each panel. Lanes C/T/A/G depict the corresponding DNA sequence.

end of the first β-strand contacts R407 in the loop, which in turn interacts with the WH domain of Prp43p (7). DHX29 also contains tyrosine (Y956) at this position, which potentially could interact with Q964 at the position equivalent to R407 in Prp43p, influencing its interaction with the WH domain. Thus, Y956 was replaced by alanine to investigate its importance for maintaining a proper interaction of the β-hairpin with the WH domain and, as a result, for DHX29's function. The neighboring K955, which also might be involved in interaction with the WH domain, was similarly replaced by alanine. The resulting K955A+Y956A double mutant retained the ability to bind to 43S complexes (Fig. 4*C*) but had very strongly reduced NTPase activity (Fig. 4*B* and *SI Appendix*, Fig. S6) and was inactive in 48S complex formation (Fig. 4*F*, lane 10), thus validating the importance of this structural element and its potential interaction with the WH domain for DHX29's function.

Large Insert in the RecA2 Domain Functions to Suppress DHX29's Intrinsic NTPase Activity. The RecA2 domains of DHX29 and other RHA-like helicases contain inserts at analogous positions, between the β1 strand and α1 helix (Fig. 1*A* and *SI Appendix*, Fig. S3). The location (Fig. 1*C*) is interesting because it is very close to the entrance of the putative RNA-binding tunnel suggested by

analogy with Ski2-like DNA helicases (9). Interestingly, although the inserts are of variable size and possess very little sequence similarity, they all contain extended stretches of charged amino acids (*SI Appendix*, Fig. S3). The PHYRE server predicts that although the 56-aa–long insert in RHA is largely unstructured, the 76-aa–long insert in DHX29 has the potential to form βαββα secondary structure elements, with the α helices being strongly predicted (Fig. 5*A*). To determine the role of the RecA2 insert in DHX29 function, we investigated the activity of four mutants. In the first mutant, five consecutive glutamate residues (789–793) were replaced by alanines; the other three mutants contained deletions of different lengths (amino acids 781–801, 781–815, and 772–820, respectively) which eliminated various predicted secondary structure elements as well as the stretch of glutamate residues (Fig. 5*A*). All mutants were active in 48S complex formation, and only initiation complexes with canonical toe-prints were observed in their presence (Fig. 5 *B* and *C*). However, all four mutants had a substantially increased level of basal NTPase activity compared with the WT protein (Fig. 5*D*), indicating that the insert has a role in suppressing DHX29's intrinsic NTPase activity. The only common features of these mutants was the absence of the stretch of glutamate residues. The fact that they all showed a similar phenotype underlines the importance of this motif for DHX29 function.

Mutational Analysis of the Predicted Ratchet Helix. It has been proposed that stacking interaction between R592 and W599 in the ratchet helix of Hel308 and DNA bases in the unwound strand of the nucleic acid duplex would play an important role in processive translocation of the enzyme along this strand during unwinding (Fig. 6*A*) (9). The positions of basic residues in the Prp43p ratchet helix differ from those in Hel308, but nevertheless a similar role was suggested for R616 and R625 (Fig. 6*A*) (8). Based on the DHX29 model, we identified R1168, R1178, and K1183 as residues that might interact with bases of the unwound RNA strand (Fig. 6*A*). Although their orientations also differ from those of R592 and W599 in DNA-bound Hel308 (Fig. 6*A*), the ratchet helix might undergo reorientation on binding of NTP and accommodation of an RNA substrate, as suggested for Prp43p (16). However, substitution of these residues individually or in combination did not influence DHX29's NTPase activity (shown for the R1168A+K1183A double mutant in Fig. 6*B*) or its function in 48S complex formation (Fig. 6 *C* and *D*). Because DHX29 is not a processive helicase (2), the ratchet helix mutants were not tested in the helicase assay.

C-Terminal Region Comprising the OB Domain and the Following Amino Acids Is Essential for the Inducibility of DHX29's NTPase Activity and for Its Function in 48S Complex Formation. The C-terminal part of DHX29 comprises the OB domain, which is connected to the ratchet domain by an α-helix and is positioned at the entrance of the putative RNA-binding tunnel, and the following C-terminal region, which is more homologous to the equivalent region in RHA-like helicases (~56% similarity with RHA) than in Prp43p (~36% similarity) (Fig. 7*A* and SI *Appendix*, Fig. S2). The PHYRE server predicts that these regions in DHX29 and other RHA-like helicases could form a series of β-strands followed by two long α-helices (Fig. 7*A* and *SI Appendix*, Fig. S2). Attempts to obtain DHX29 mutants lacking the last α-helix ($DHX29_{1–1350}$), both C-terminal α-helices ($DHX29_{1–1327}$), or the entire region following the OB domain ($DHX29_{1–1291}$) (Fig. 7*A*) yielded polypeptides that were much less soluble than WT DHX29 and that eluted over the entire gradient rather than as a single peak during MonoQ or MonoS chromatography. Although these mutants were not active in 48S complex formation, their physical characteristics suggest that they were likely misfolded, and therefore they are not discussed further. In contrast, the DHX29 mutant lacking the C-terminal region up to the α-helix connecting the OB and ratchet domains ($DHX29_{1–1227}$) was soluble and eluted as a single peak from MonoQ and MonoS columns. Although deletion of this region did not affect ribosomal binding of DHX29 (Fig. 7*B*), the NTPase activity of $DHX29_{1–1227}$ was not stimulated by either 40S subunits or U_{70} (Fig. 7*C*), and this mutant also was inactive in 48S complex formation (Fig. 7*D*). These results indicate that the C-terminal region starting from the OB domain is required to render DHX29's NTPase activity responsive to stimulation and that such responsiveness is essential for its function in 48S complex formation. Interestingly, like the RecA2-insert mutants, $DHX29_{1–1227}$ had elevated basal NTPase activity, which suggests that the OB domain and the

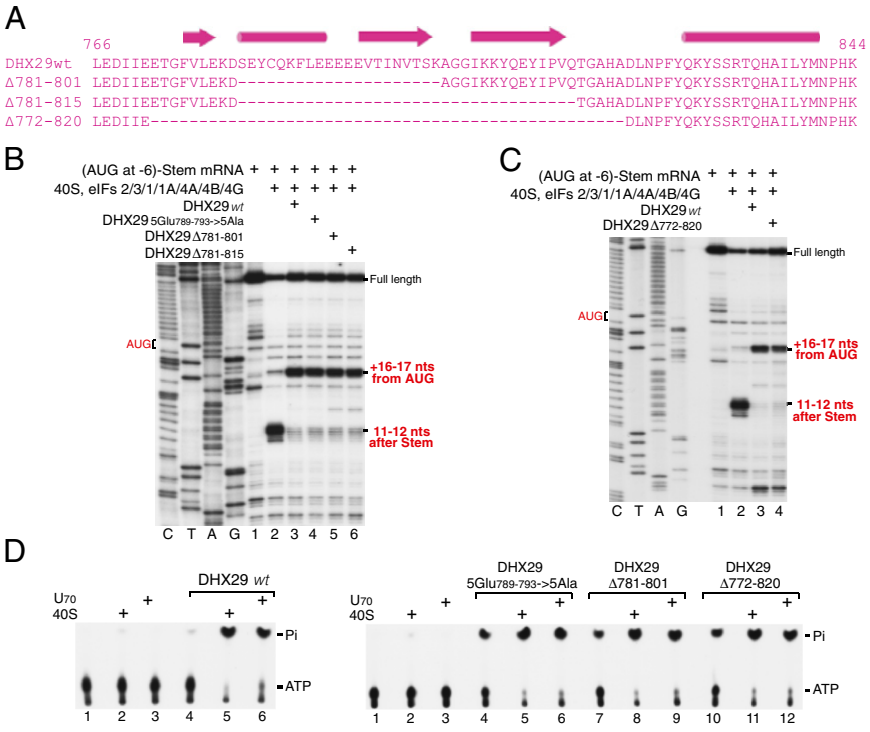

Fig. 5. Mutations in the insert in the RecA2 domain increase DHX29's intrinsic NTPase activity. (*A*) Amino acid sequence of the insert in DHX29's RecA2 domain showing predicted secondary structure elements and residues deleted in RecA2-insert mutants. (*B* and *C*) Toe-printing analysis of the activity of RecA2-insert mutants in promoting 48S complex formation on (AUG at −6)-Stem mRNA. Initiation codons and the positions of full-length cDNA and of assembled ribosomal complexes are shown on the sides of each panel. Lanes C/T/A/G depict the corresponding DNA sequence. (*D*) TLC analysis of the NTPase activity of the RecA2-insert mutants in the presence of 40S subunits and U_{70} RNA. The positions of [^{32}P]-ATP and [^{32}P]-P_i are shown on the right.

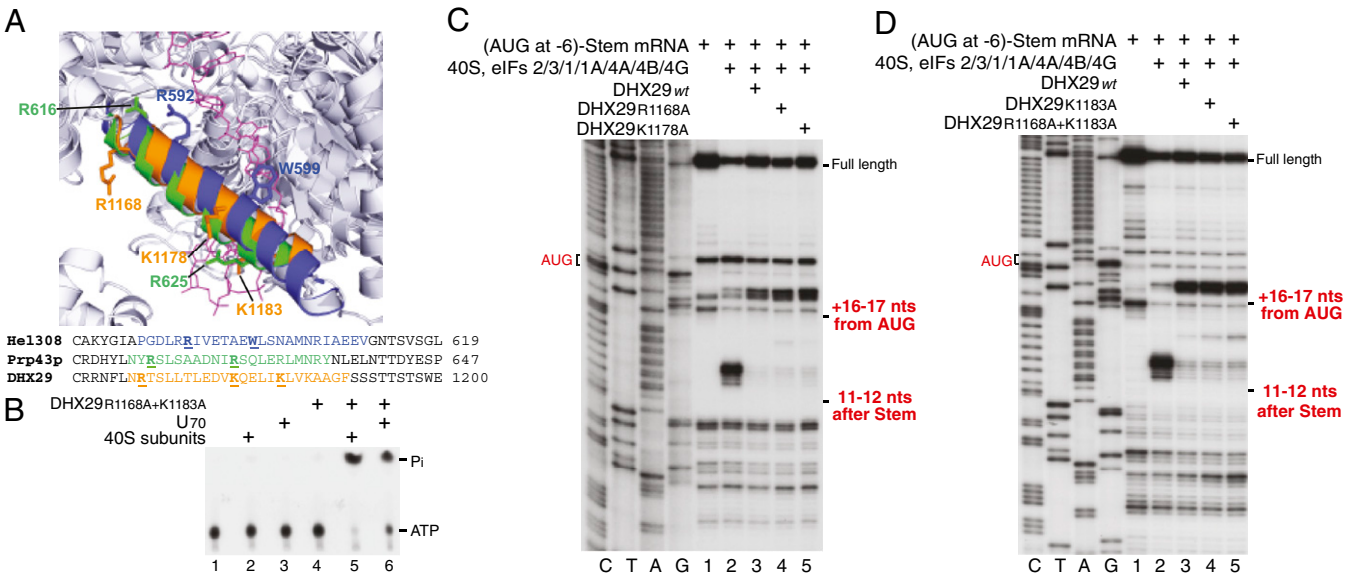

Fig. 6. Mutational analysis of DHX29's predicted ratchet helix. (*A*) (*Upper*) Superposition of the ratchet helices from the Hel308/DNA complex (PDB ID: 2P6R) (blue), Prp43p (PDB ID: 3KX2) (green), and DHX29 (predicted model) (orange). DNA is shown as magenta sticks. (*Lower*) Amino acid sequences of the ratchet helices from Hel308, Prp43p, and DHX29. Potential residues that could interact with bases of the unwound RNA/DNA strands are labeled on the *Upper* panel and underlined on the *Lower* panel. (*B*) TLC analysis of the NTPase activity of a representative ratchet helix mutant in the presence of 40S subunits and U_{70} RNA, as indicated. The positions of [^{32}P]-ATP and [^{32}P]-P_i are shown on the right. (*C* and *D*) Toe-printing analysis of the activity of the ratchet helix mutants in promoting 48S complex formation on (AUG at −6)-Stem mRNA. Initiation codons and the positions of full-length cDNA and of assembled ribosomal complexes are shown on the sides of each panel. Lanes C/T/A/G depict the corresponding DNA sequence.

following region play an autoinhibitory role in suppressing DHX29's intrinsic NTPase activity.

Discussion

Determinants of DHX29's Ribosomal Association. The accessory domains flanking the catalytic RecA cores of SF1 and SF2 helicases determine their diverse physiological functions by interacting with specific RNAs, DNAs, or proteins that modulate their activities and tie a given helicase to a distinct biological process. Thus, Prp43p binds to the activating protein Pfa1p via interactions involving C-terminal elements (e.g., ref. 8), Prp16p and Prp22p contain determinants of spliceosome interaction in their N-terminal regions (17, 18), and a unique N-terminal domain enables DHX36 to bind to guanine-quadruplex RNAs (19). We found that targeting of DHX29 to 43S complexes depends on elements that map to the DHX29-specific NTR and to the N-terminal half of the WH domain, which includes the α1/α2 helices and the α2-α3 loop. The essential determinant in the NTR was identified as a putative dsRBD (amino acids 377–448), a motif that occurs only in a few DExH-box helicases, including RHA and its homologs, such as *Drosophila maleless* (MLE). The N-terminal regions of RHA/MLE contain tandem dsRBDs, and although their relative contributions to RNA-binding activity have not been fully resolved, deletion of dsRBD2 abrogates productive engagement of RHA and MLE with their specific RNA substrates (e.g., refs. 20–22). Deletion of the dsRBD in DHX29 abrogated ribosomal association and ribosomal stimulation of its NTPase activity and abolished its function in 48S complex formation, even though it did not affect stimulation of DHX29's NTPase activity by RNA. Thus, specific targeting of DHX29 to 40S subunits is essential for its role in initiation. Importantly, although deletion of the dsRBD resulted in a total loss of ribosomal association, removal of the entire NTR did not abrogate ribosomal binding, and the resulting protein possessed ribosome-stimulated NTPase activity (albeit at a reduced level) and residual activity in 48S complex formation. These results suggest that the dsRBD likely mediates the primary ribosomal contact, whereas interaction with the WH domain is secondary, and in intact DHX29 this site might become accessible only after conformational changes induced by the establishment of the primary interaction.

WH domains constitute a conserved module within similar structural units in many SF2 helicases, but their role in helicase function remains obscure. Although WH domains often bind to DNA, and their specificity is determined by residues in α3 (23), no interaction between the WH domain and DNA was apparent in the crystal structure of DNA-bound Hel308 (9). However, it has been suggested that the position of the WH domain and the surface-exposed location of its α1 and α3 helices would be suitable for binding to Hel308-interacting proteins (e.g., *Sulfolobus* Hjc), and, notably, conserved aromatic residues in its α1/α2 helices were found to be functionally important (24). Thus, the interaction of DHX29's WH domain with 40S subunits provides evidence that WH domains of SF2 helicases indeed could be involved in direct interaction with their functional partners. Even though the interaction between 40S subunits and the WH domain might depend on the initial interaction established by the dsRBD, direct contact of the WH domain with the 40S subunit might be crucial for stimulation of DHX29's NTPase activity, taking into account the extensive interaction between the WH and RecA1 domains in Prp43p (7, 8) and also, probably, in DHX29.

RecA Catalytic Core. DHX29 contains eight conserved motifs in the RecA1 and RecA2 domains (Fig. 4*A*). Mutations in motifs I, II, V, and VI abolished DHX29's NTPase activity, comparable to the effects of analogous mutations in Prp16p, Prp22p, and Prp43p (25–27). The loss of NTPase activity correlated with the inability of DHX29 mutants to promote 48S complex formation on structured mRNA, confirming that NTP hydrolysis is required for DHX29's function in the initiation process. A triple substitution in motif III completely abrogated DHX29's function in 48S complex formation but had only a small effect on its NTPase activity, as is consistent with the suggested role of this motif in coupling NTP hydrolysis with unwinding of RNA or remodeling of ribonucleoprotein complexes (e.g., ref. 15).

Like other DExH-box helicases, DHX29 contains a β-hairpin protruding from between motifs V and VI in the RecA2 domain. In the crystal structure of ADP-bound Prp43p, the β-hairpin is

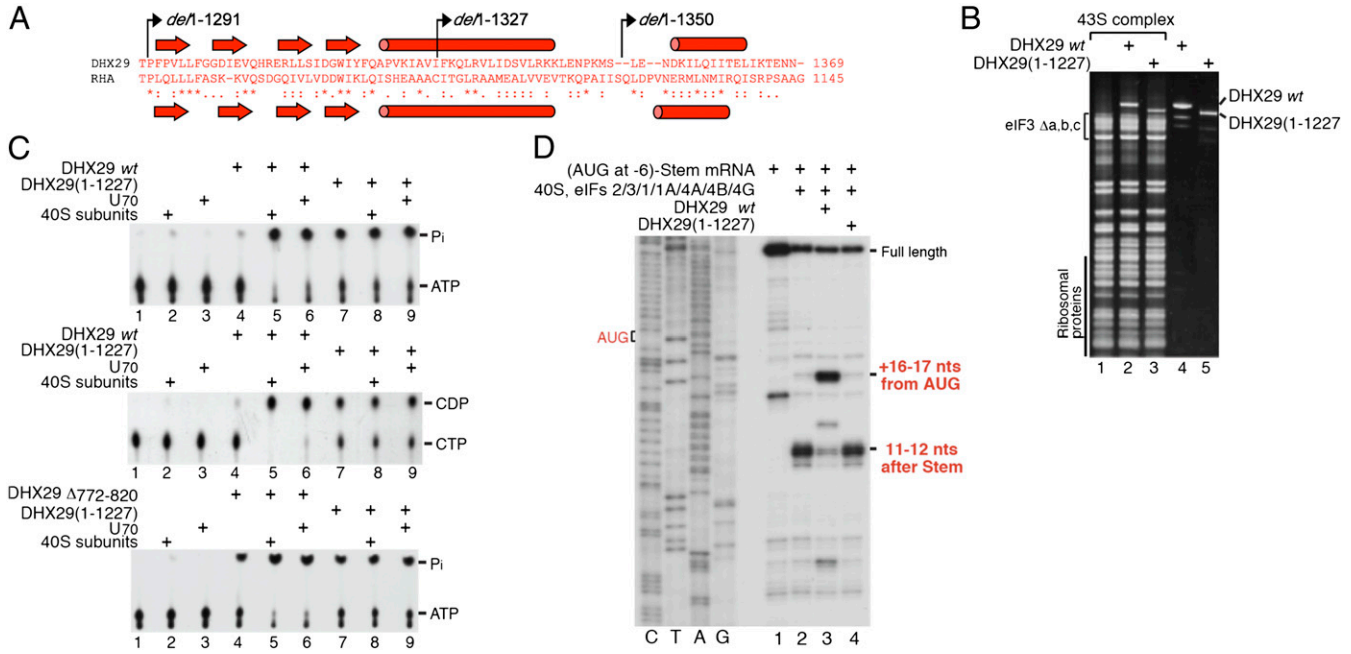

Fig. 7. The C-terminal region is essential for inducibility of DHX29's NTPase activity and for its function in 48S complex formation. (*A*) Alignment of amino acid sequences of the C-terminal regions of DHX29 and RHA, showing predicted secondary structure elements. The boundaries of C-terminal deletions in DHX29 are marked by arrows. (*B*) Association of the DHX29$_{1–1227}$ truncation mutant with 43S complexes. After incubation with DHX29, ribosomal complexes were separated by SDG centrifugation, and DHX29's presence in ribosomal peak fractions was analyzed by SDS/PAGE and fluorescent SYPRO staining. (*C*) TLC analysis of the NTPase activity of the DHX29$_{1–1227}$ truncation mutant and a RecA2-insert mutant in the presence of 40S subunits and U_{70} RNA. The positions of [^{32}P]-ATP, [^{32}P]-P$_i$, [^{32}P]-CTP, and [^{32}P]-CDP are shown on the right. (*D*) Toe-printing analysis of the activity of the DHX29$_{1–1227}$ truncation mutant in promoting 48S complex formation on (AUG at −6)-Stem mRNA. Initiation codons and the positions of full-length cDNA and of assembled ribosomal complexes are shown on the side of the panel. Lanes C/T/A/G depict the corresponding DNA sequence.

inserted in a cleft between the WH and OB domains and, with the β4-β5 loop of the OB domain, occludes the putative ssRNA entrance (7, 8). Therefore it was suggested that, to open the ssRNA-binding pocket, upon binding to ATP, Prp43p would have to undergo substantial rearrangement involving rotation of RecA2, WH, and OB domains, accompanied by movements of the tip of the β-hairpin and of the β4–β5 loop of the OB domain (7, 16). Thus, the loss of the NTPase and translational activities of DHX29 caused by KY$_{955–956}$/AA substitutions in the apex of its predicted β-hairpin, which in the case of Prp43p is involved in interaction with the WH domain, might be caused by the disruption of a similar, functionally important interaction among the RecA2, WH, and OB domains of DHX29, integrated by the β-hairpin.

The RecA1/RecA2 core domains of several helicases belonging to all three SF1 and to two of the nine SF2 families contain independently folded inserts that have little effect on the structure of the core domain but are critical for biological function (28). Thus, deletion of the 1B and 1C inserts from Upf1's RecA1 domain impaired its RNA binding and abrogated the negative cooperativity between binding of ATP and RNA, respectively (29); deletion of the 1B domain of RecD abrogated its helicase activity, uncoupling it from its ATPase activity (30); whereas the insert in the RecA2 domain of the *E. coli* Rep protein instead acts as an autoinhibitory repressor of its helicase activity (31). We found that the large insert between β1 and α1 of the RecA2 domain of DHX29 is required for suppression of its basal intrinsic NTPase activity but is not essential for stimulation of DHX29's NTPase activity by 40S subunits or by RNA or for its function in initiation. The fact that substitution of five consecutive glutamate residues in the insert had an effect similar to that of major deletions in it suggests that this motif might be important for the structural integrity of the insert or for its interaction with other domains to maintain DHX29 in a repressed conformation. Importantly, all other RHA-like helicases contain inserts at the analogous location (*SI Appendix*, Fig. S3), so it would be interesting to investigate whether their NTPase activities are regulated by these inserts in a similar manner.

Ratchet Domain. Substitution of residues in DHX29's predicted ratchet helix, which potentially could interact with the bases of the unwound RNA strand to facilitate translocation of DHX29 along it, did not influence DHX29's function in 48S complex formation. This observation would be consistent with DHX29's lacking processive helicase activity (2) and its functioning by remodeling 43S complexes at the mRNA entrance rather than by direct unwinding of mRNAs before they enter the mRNA-binding cleft. However, because we cannot strictly exclude the possibility that modeling did not identify correctly the residues involved in interaction with the unwound RNA, it remains possible that binding to 43S complexes strongly enhances DHX29's helicase activity, allowing it to participate in direct unwinding.

Essential Role of the OB Domain in DHX29's NTPase Activity. The C terminus of DHX29 comprises the OB domain followed by a region that is predicted to form a series of β-strands followed by two α-helices. C-terminal truncations that removed various elements or the entire region after the OB domain strongly reduced the yields of soluble proteins, which in addition showed characteristics of misfolding. However, further C-terminal truncation that also removed the OB domain yielded a soluble protein that retained the ability to bind to 40S subunits, suggesting that the OB domain and the following C-terminal region form a single structural unit. A DHX29 mutant lacking the OB domain and the C-terminal region could no longer respond to stimulation by 40S subunits or by RNA in the NTPase assay and was inactive in 48S complex formation. Similar C-terminal truncation in Prp43p also impaired the stimulation of its ATPase activity by RNA (8). The facts that the regions following the OB domain in DHX29 and Prp43p are not obviously related and that similar effects on the NTPase activity of Prp43p were observed for the OB domain substitution mutants

suggest that in both proteins this domain is primarily responsible for the responsiveness of their NTPase activities to stimulation. Importantly, although the OB domain is positioned near the putative mRNA entrance, and the interaction with RNA of a Prp43p deletion mutant lacking this domain was reduced, some mutations in Prp43p's OB domain that did not influence its RNA-binding activity nevertheless impaired stimulation of its ATPase activity by RNA (8). Moreover, in the case of DHX29, a similar truncation resulted in the loss of both RNA- and 40S-mediated stimulation of NTPase activity, even though this mutant retained the ability to bind to 40S subunits. This result suggests that the OB domain not only influences binding of DExH/RHA helicases to RNA but also is actively involved in their NTPase cycle.

Interestingly, deletion of the OB domain and the following region not only impaired the stimulation of DHX29's NTPase activity by RNA or by 40S subunits but also increased its intrinsic NTPase activity, similar to the effects of mutations in the RecA2 insert. Like the OB domain, the insert probably is positioned near the mRNA entrance and therefore might interact directly with the C-terminal unit, allowing these elements to cooperate in suppressing DHX29's intrinsic NTPase activity. High-resolution structures of ATP- and ADP-bound states of DHX29 depending on the presence of RNA will be required to understand the mechanism by which the C-terminal elements and RecA2 domain inserts of this and other DEAH/RHA helicases fulfill their function in regulating the NTPase cycle.

Materials and Methods

Plasmids and preparation of initiation factors and 40S ribosomal subunits are described in *SI Appendix*.

Analysis of Ribosomal Association of DHX29. To investigate ribosomal binding of DHX29 in stringent conditions of SDG centrifugation, 60 pmol DHX29 were incubated with 30 pmol 40S subunits, 60 pmol eIF2, 40 pmol eIF3, 100 pmol eIF1, 100 pmol eIF1A, and 60 pmol Met-tRNA$_i^{Met}$ in 200-μL reaction mixtures containing buffer A [20 mM Tris (pH 7.5), 100 mM KCl, 2.5 mM $MgCl_2$, 2 mM DTT, and 0.25 mM spermidine] supplemented with 1 mM ATP and 0.4 mM GTP at 37 °C for 10 min. The reaction mixtures then were subjected to centrifugation through a 10–30% (wt/wt) SDG prepared in buffer A in a Beckman SW55 rotor at 53,000 rpm for 1 h 15 min. Fractions that corresponded to 43S ribosomal complexes were analyzed by SDS/PAGE with subsequent fluorescent SYPRO (Molecular Probes) staining or Western blotting using DHX29 (Bethyl Laboratories) or FLAG-tag (Sigma-Aldrich) antibodies.

To assay the relative ribosomal-binding activities of WT and mutant DHX29 in concentrations of translational components analogous to those used in 48S complex formation, centrifugation through a sucrose cushion was used (32). For this process, 50-μL reaction mixtures containing 2 pmol 40S subunits, 5 pmol Met-tRNA$_i^{Met}$, 3 pmol eIF2, 2 pmol eIF3, 12 pmol eIF1, 8 pmol eIF1A, and 0.3 pmol WT or mutant DHX29 in buffer A supplemented with 1 mM ATP and 0.4 mM GTP were incubated for 10 min at 37 °C, layered onto ice-cold 50-μL sucrose cushions (10% sucrose in buffer A), and centrifuged at 4 °C for 13 min at 90,000 rpm in a Beckman TLA 120.1 rotor. The unbound fraction was obtained by removing 65-μL aliquots from the supernatant, and the bound fraction was obtained by dissolving the ribosomal pellet in the remaining 35 μL of the reaction mixture. These aliquots were analyzed by SDS/PAGE with subsequent fluorescent SYPRO (Molecular Probes) staining.

NTPase Assay. To investigate the NTPase activity of DHX29 mutants, 0.15 pmol of WT or mutant DHX29 was incubated with 6.7 μM [γ-^{32}P]ATP or [α-^{32}P]CTP in the presence or absence of 2 pmol 40S subunits or 20 pmol U_{70} RNA in a 10-μL reaction mixture containing buffer A at 37 °C for 15 min. Then 2-μL aliquots were spotted onto polyethyleneimine cellulose plates for chromatography done using 0.8 M LiCl/0.8 M acetic acid. The NTPase activity was determined by formation of [^{32}P]-P_i or [α-^{32}P]-CDP.

Toe-Printing Analysis. 48S complexes were assembled on uncapped in vitro-transcribed (AUG at −6)-Stem mRNA. Forty-microliter reaction mixtures containing 1 pmol mRNA, 2 pmol 40S subunits, 5 pmol Met-tRNA$_i^{Met}$, 3 pmol eIF2, 2 pmol eIF3, 12 pmol eIF1, 8 pmol eIF1A, 8 pmol eIF4A, 1.5 pmol eIF4B, 6 pmol eIF4G$_{457–932}$, and 0.3 pmol DHX29 in buffer A supplemented with 1 mM ATP and 0.4 mM GTP were incubated for 10 min at 37 °C. Assembled initiation complexes were analyzed by primer extension using Avian myeloblastosis virus reverse transcriptase (Promega) and a [^{32}P]-labeled primer complementary to the coding region of (AUG at −6)-Stem mRNA. cDNA products were resolved in 6% polyacrylamide sequencing gels.

ACKNOWLEDGMENTS. This work was funded by National Institutes of Health Grant GM59660 (to T.V.P.).

1. Jackson RJ, Hellen CU, Pestova TV (2010) The mechanism of eukaryotic translation initiation and principles of its regulation. *Nat Rev Mol Cell Biol* 11(2):113–127.
2. Pisareva VP, Pisarev AV, Komar AA, Hellen CU, Pestova TV (2008) Translation initiation on mammalian mRNAs with structured 5′UTRs requires DExH-box protein DHX29. *Cell* 135(7):1237–1250.
3. Skabkin MA, et al. (2010) Activities of Ligatin and MCT-1/DENR in eukaryotic translation initiation and ribosomal recycling. *Genes Dev* 24(16):1787–1801.
4. Yu Y, et al. (2011) The mechanism of translation initiation on Aichivirus RNA mediated by a novel type of picornavirus IRES. *EMBO J* 30(21):4423–4436.
5. Parsyan A, et al. (2009) The helicase protein DHX29 promotes translation initiation, cell proliferation, and tumorigenesis. *Proc Natl Acad Sci USA* 106(52):22217–22222.
6. Abaeva IS, Marintchev A, Pisareva VP, Hellen CU, Pestova TV (2011) Bypassing of stems versus linear base-by-base inspection of mammalian mRNAs during ribosomal scanning. *EMBO J* 30(1):115–129.
7. He Y, Andersen GR, Nielsen KH (2010) Structural basis for the function of DEAH helicases. *EMBO Rep* 11(3):180–186.
8. Walbott H, et al. (2010) Prp43p contains a processive helicase structural architecture with a specific regulatory domain. *EMBO J* 29(13):2194–2204.
9. Büttner K, Nehring S, Hopfner KP (2007) Structural basis for DNA duplex separation by a superfamily-2 helicase. *Nat Struct Mol Biol* 14(7):647–652.
10. Schütz P, et al. (2010) Crystal structure of human RNA helicase A (DHX9): Structural basis for unselective nucleotide base binding in a DEAD-box variant protein. *J Mol Biol* 400(4):768–782.
11. Kelley LA, Sternberg MJE (2009) Protein structure prediction on the Web: A case study using the Phyre server. *Nat Protoc* 4(3):363–371.
12. Chang KY, Ramos A (2005) The double-stranded RNA-binding motif, a versatile macromolecular docking platform. *FEBS J* 272(9):2109–2117.
13. Ramos A, et al. (2000) RNA recognition by a Staufen double-stranded RNA-binding domain. *EMBO J* 19(5):997–1009.
14. Nanduri S, Carpick BW, Yang Y, Williams BR, Qin J (1998) Structure of the double-stranded RNA-binding domain of the protein kinase PKR reveals the molecular basis of its dsRNA-mediated activation. *EMBO J* 17(18):5458–5465.
15. Schwer B, Meszaros T (2000) RNA helicase dynamics in pre-mRNA splicing. *EMBO J* 19 (23):6582–6591.
16. He Y, Andersen GR, Nielsen KH (2011) The function and architecture of DEAH/RHA helicases. *BioMolecular Concepts* 2:315–326.
17. Wang Y, Guthrie C (1998) PRP16, a DEAH-box RNA helicase, is recruited to the spliceosome primarily via its nonconserved N-terminal domain. *RNA* 4(10):1216–1229.
18. Schneider S, Schwer B (2001) Functional domains of the yeast splicing factor Prp22p. *J Biol Chem* 276(24):21184–21191.
19. Lattmann S, Giri B, Vaughn JP, Akman SA, Nagamine Y (2010) Role of the amino terminal RHAU-specific motif in the recognition and resolution of guanine quadruplex-RNA by the DEAH-box RNA helicase RHAU. *Nucleic Acids Res* 38(18):6219–6233.
20. Zhang S, Grosse F (1997) Domain structure of human nuclear DNA helicase II (RNA helicase A). *J Biol Chem* 272(17):11487–11494.
21. Izzo A, Regnard C, Morales V, Kremmer E, Becker PB (2008) Structure-function analysis of the RNA helicase maleless. *Nucleic Acids Res* 36(3):950–962.
22. Ranji A, Shkriabai N, Kvaratskhelia M, Musier-Forsyth K, Boris-Lawrie K (2011) Features of double-stranded RNA-binding domains of RNA helicase A are necessary for selective recognition and translation of complex mRNAs. *J Biol Chem* 286(7): 5328–5337.
23. Gajiwala KS, Burley SK (2000) Winged helix proteins. *Curr Opin Struct Biol* 10(1):110–116.
24. Woodman IL, Bolt EL (2011) Winged helix domains with unknown function in Hel308 and related helicases. *Biochem Soc Trans* 39(1):140–144.
25. Martin A, Schneider S, Schwer B (2002) Prp43 is an essential RNA-dependent ATPase required for release of lariat-intron from the spliceosome. *J Biol Chem* 277(20): 17743–17750.
26. Schneider S, Hotz HR, Schwer B (2002) Characterization of dominant-negative mutants of the DEAH-box splicing factors Prp22 and Prp16. *J Biol Chem* 277(18): 15452–15458.
27. Tanaka N, Schwer B (2006) Mutations in PRP43 that uncouple RNA-dependent NTPase activity and pre-mRNA splicing function. *Biochemistry* 45(20):6510–6521.
28. Fairman-Williams ME, Guenther UP, Jankowsky E (2010) SF1 and SF2 helicases: Family matters. *Curr Opin Struct Biol* 20(3):313–324.
29. Cheng Z, Muhlrad D, Lim MK, Parker R, Song H (2007) Structural and functional insights into the human Upf1 helicase core. *EMBO J* 26(1):253–264.
30. Saikrishnan K, Griffiths SP, Cook N, Court R, Wigley DB (2008) DNA binding to RecD: Role of the 1B domain in SF1B helicase activity. *EMBO J* 27(16):2222–2229.
31. Brendza KM, et al. (2005) Autoinhibition of Escherichia coli Rep monomer helicase activity by its 2B subdomain. *Proc Natl Acad Sci USA* 102(29):10076–10081.
32. Shin BS, et al. (2002) Uncoupling of initiation factor eIF5B/IF2 GTPase and translational activities by mutations that lower ribosome affinity. *Cell* 111(7): 1015–1025.